

EXPERIMENTAL MEASUREMENT AND FINITE ELEMENT ANALYSIS OF SCREW SPIKE FATIGUE LOADS

Matthew G. Dick
David S. McConnell
Hans C. Iwand
Rail Sciences, Inc.

ABSTRACT

Screw spikes, also known as coach screws, are an advanced alternative to common cut spikes for track fastening. Despite their ability to secure tie plates with a clamp load and utilization of high strength steels, they are still susceptible to bending fatigue failure from lateral wheel loads. A novel method of measuring these bending loads on screw spikes was developed and implemented to characterize the load environment of the screw spikes. Results indicated that measured peak bending loads under lateral wheel loads reached as high as 10,000 lbs for individual spikes, while others carried no load whatsoever. A finite element model was developed to determine the tensile stress fields created by the measured bending loads. A good correlation was found between the FEA model predicted point of highest stress and the location of fracture. Through the testing and analysis it was determined that lateral wheel loads are not distributed evenly among the four screw spikes of a single tie plate. Instead, it was found that one spike carried nearly no load while the spike opposite of it carried more load. Using the finite element analysis it was determined that the spike exposed to the higher loading was subjected to tensile stresses above its endurance limit, which would eventually lead to a bending fatigue failure.

INTRODUCTION

Much like other railroad components, screw spikes have undergone an increase of failures due to a change of their load environments. This change can be attributed to ever increasing railcar wheel loads and total trailing tonnage in combination to an aging track structure. The primary goal of this research was to investigate the load environment for screw spikes to help understand their failures.

Screw spikes, also known as coach screws, are another method of track fastening to more common cut spikes. Their purpose is to provide lateral fastening support from rail to wood ties. Unlike cut spikes, screw spikes can provide a clamp load onto the tie plates by their inherent screw design. This helps to reduce tie plate movement and prevent a "raised spike" condition typical of cut spikes. Despite their design, they have proved to still be susceptible to failure.

Screw spikes fail due to bending fatigue from rail vehicle lateral wheel loads. New and failed screw spikes are shown in

Fig 1. Figure 2 is the fatigue fracture surface of a typical failed screw spike. Each failed screw spike fracture surface contains the three stages of fatigue. First the crack originates from one or two thread lengths from the top, at a root diameter reduction. Secondly, the fatigue crack progresses through the cross-section of the spike. Note the characteristic beach marks which indicate the crack direction and bending loads. Once the fatigue crack has grown to significantly reduce the screw spike's strength, a final overload failure occurs. The crack growth portion of the fracture indicated a high cycle – low stress condition that allowed the fatigue crack to grow to approximately 80% of the cross-section. Failed screw spikes most frequently are found in high degree curves where rail vehicles have their highest lateral wheel loads.



Figure 1. Overview of new and failed screw spikes.

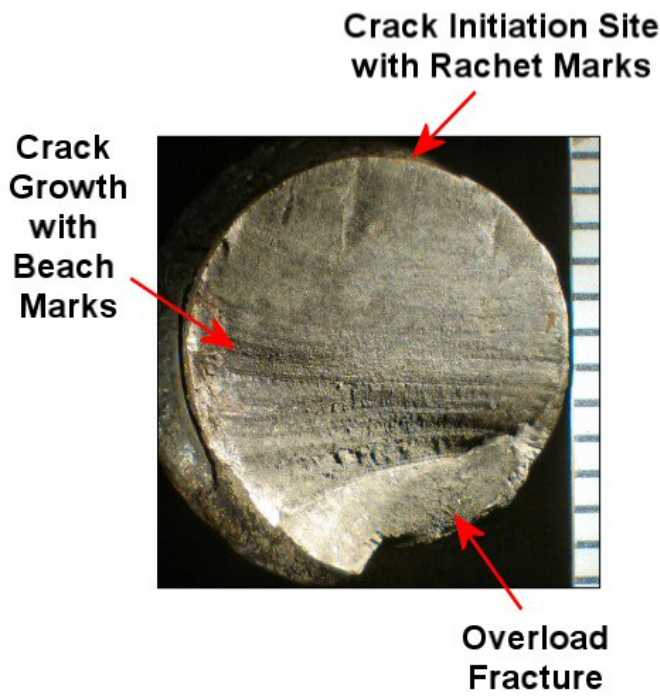


Figure 2. Overview of fracture surface. Scale graduations are one-sixteenths of an inch.

MATERIAL EVALUATION

Chemical composition, tensile, and hardness tests were performed of the high-strength screw spike material. Results of the chemistry analysis are shown in Table 1 and indicated a low-carbon, low-alloy steel. Results of the tensile and hardness tests are shown in Table 2. The manufacturer specification requires a minimum tensile strength of 120 ksi (827 MPa), which the tested material met. The material also met the tensile requirements outlined in ASTM A66 – Standard Specification for Steel Screw Spikes. A simplified endurance limit of 72 ksi (496 MPa) was estimated as 60% of the minimum tensile strength.

Element	Ave wt%
C	0.192
P	0.009
S	0.011
Mn	0.869
Si	0.340
Cr	0.125
Mo	0.031
Ni	0.147
Cu	0.338
V	0.006
Al	0.051

Table 1. Screw spike chemical composition results.

Material Property	Value
Upper Yield Strength	97.8 ksi (674 MPa)
Lower Yield Strength	94.9 ksi (654 MPa)
Tensile Strength	131.5 ksi (907 MPa)
% Elongation	18.1%
Hardness	30.5 HRC

Table 2. Screw spike material tensile and hardness results.

INSTRUMENTED SCREW SPIKE DESIGN

It was desired to measure lateral loads using the screw spikes themselves to not disrupt the track system. This was accomplished by designing a strain gauge based load cell which could be applied to a normal screw spike, which is shown in Fig 3. This method used a flexural beam insert instrumented with a strain gauge. A hole was bored through the head of the screw at which the flexural beam could be inserted. Whenever the screw spike would bend, this would create an identical bend in the flexural beam which would be indicated by the strain gauge. This design protected the instrumentation within the body of screw and allowed for normal installation using a specialty socket and hydraulic impact wrench. A total of seven instrumented screw spikes were constructed at the Rail Sciences laboratory.

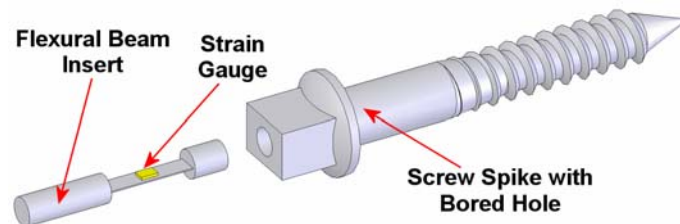


Figure 3. Instrumented screw spike design.

CALIBRATION

Each screw spike was initially calibrated using a MTS servo-hydraulic actuator at the Rail Sciences laboratory in Omaha, NE. Screw spikes were installed two at a time into a shortened wood tie. Tie plates were replaced with brackets with holes for the screws to pass through, but could also be held by the two hydraulic actuator grips. Washers were added as needed to maintain the correct height of a nominally installed screw spike. Screw spikes were installed so that the flexural beam was perpendicular to the applied load. During calibration it was observed that the freshly drilled holes in the test wood tie performed differently over numerous cycles. For this reason, the final calibration was not taken until each drilled hole had been “broken in” and had reached a steady state of screw spike support. Using the calibrated MTS displacement and load measurement capabilities, load vs. microstrain, displacement vs. microstrain, and load vs. displacement curves were created for each screw spike.

During the on-site test it was observed that the wood tie condition was significantly different than the wood tie used during laboratory calibration. The stiffness of the wood tie around the screw spike was found to be very influential to screw spike bending. It was determined that the laboratory calibration alone was not sufficient to accurately calibrate the

on-site installed screw spikes. A second method of calibration was performed using a finite element model of the instrumented screw spike with the flexural beam insert. Screw spike displacement using a LVDT and microstrain were recorded during the on-site test. These parameters were used with the FEA model to determine the corresponding wood tie stiffness and applied lateral load. Measured microstrain on the flexural beam was compared to the strains predicted by the finite element model. A final composite calibration was created using the laboratory and FEA calibrations. The laboratory calibrations had shown a slight variance between the seven instrumented screw spikes. This variance was expected and can be attributed to variations of strain gauge application and flexural beam installation. The average laboratory calibration was considered the characteristic calibration for the wood tie used in the laboratory. However, the tie condition on-site was different than at the laboratory. The finite element model predicted the characteristic calibration for the on-site wood ties. For the final composite calibration each instrumented screw spike laboratory calibration was proportionally adjusted so that the average calibration equaled the FEA predicted characteristic calibration of the on-site wood ties.

TEST SITE

Instrumented screw spikes were installed at a location of recorded failures. The area was in a mountainous region and had many high degree curves with wood ties. The specific location was a 10° curve where a truck performance detector (TPD) was located. Four instrumented screw spikes were installed in a single tie plate on the high rail of the curve. This was intended to determine how the screw spikes divide the net lateral load on a tie plate. The other four instrumented screw spikes were installed as satellites from the fully instrumented tie plate. Two LVDTs were installed to measure lateral displacement of two instrumented screw spikes. Locations of the instrumentation are shown in Fig 4. An overview of the instrumented tie plate is shown in Fig 5. The screw spikes were installed so that the flexural beam was parallel to the rail.

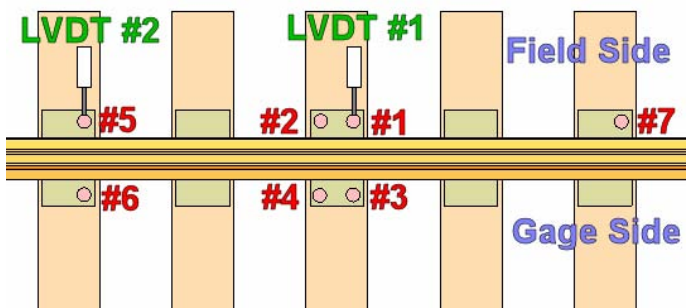


Figure 4. Schematic of instrumented screw spike and LVDT locations on the high rail of the curve.



Figure 5. Overview of fully instrumented tie plate.

Data acquisition was performed using a Somat eDAQ system recording at 200 Hz with a 50 Hz low-pass filter. Autonomous recording was accomplished by one of the LVDTs triggering a preset value. The system operated for 24 hours and recorded a total of 14 trains. A second data acquisition program was run to measure the long-term loads on screw spikes. This was measured at 0.02 Hz continuously over the course of the 24 hours. A thermal couple was attached to the rail to measure the rail temperature during this long-term testing. This second measurement program was added to investigate if significant loads lateral loads could be created on the screw spikes due to the rail cooling and contracting, causing the track to “suck in” toward the center of the curve.

TEST RESULTS

Results of the on-site testing revealed that within a single tie plate, lateral wheel loads are not evenly distributed between the four screw spikes, as indicated in Fig 6. Note that screw spike #2 carried the majority of the load while screw spike #4 carried virtually no load. Interestingly, screw spikes #2 and #4 are directly across from each other on the field and gage sides, respectively. During testing, the maximum screw spike load measured was 14,800 lbs (65.8 kN). Table 3 shows how the four screw spikes divided the net lateral load in a single tie plate. These values were determined by calculating the RMS values of the four measured channels over the course of the test. Note that screw spike #2 carried approximately 2.5 times more than the average of the screw spikes with the tie plate.

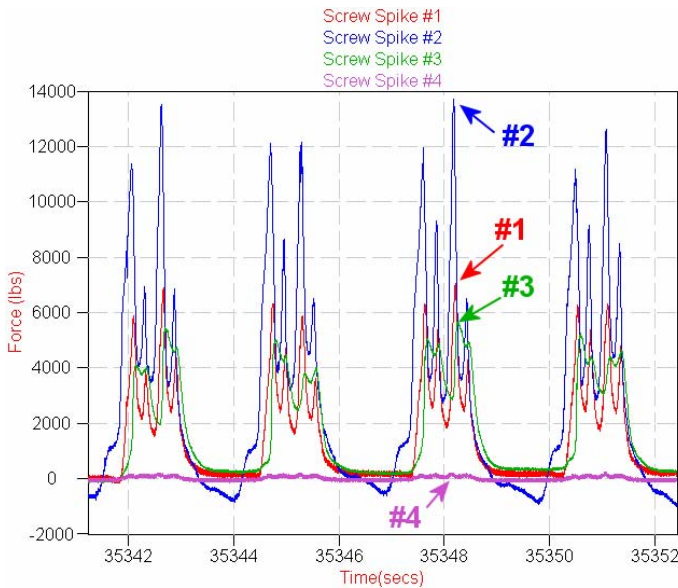


Figure 6. Characteristic plot of screw spike lateral loads in a single tie plate.

Screw Spike	Percentage of Load Carried
#1	21.3%
#2	63.1%
#3	14.6%
#4	1.0%

Table 3. Screw spike load division within a single tie plate.

Results from the LVDT indicated that screw spike movement was fairly erratic over the course of a train length, as indicated in Fig 7. This was attributed to the complex state of friction between the tie plate, tie, and the screw spikes. However, when the screw spike was in a somewhat steady-state, displacement was typically between 0.005 to 0.010 inches (0.13 to 0.25 mm).

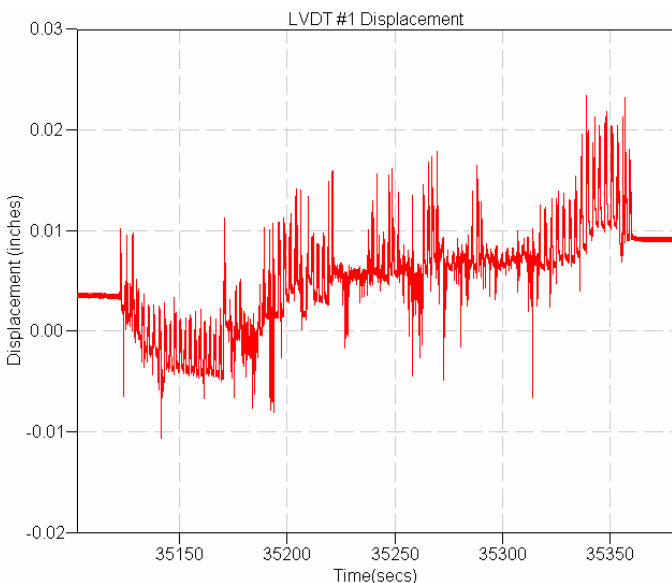


Figure 7. LVDT #1 displacement for one train.

Results of the long term testing had revealed that the screw spikes were not subjected to significant bending loads. Screw spike #4 indicated the greatest bending load from long-term temperature effects. Figure 8 is a plot comparing the lateral load on screw spike #4 and the rail temperature, which indicated a good correlation. Note that the lateral load is negative or towards the gage side. This would indicate that as the rail cooled and contracted overnight, the track shifted toward the center of the curve, applying load to screw spike #4. Interestingly, screw spike #4 carried virtually no load from rail vehicle lateral wheel loads, but did carry load from the track contracting.

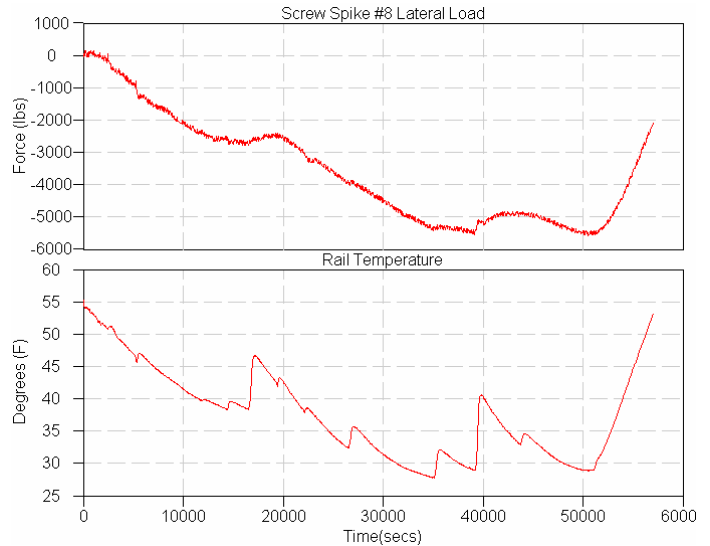


Figure 8. Screw spike #8 lateral load as compared to rail temperature.

FINITE ELEMENT STRESS ANALYSIS

After measuring screw spike lateral loads, it was necessary to calculate the resulting fatigue stresses. To accomplish this, a finite element model of a screw spike was created and analyzed using the FEA software COSMOS™. An overview of the model is shown in Fig 9. Threads of the screw were not simulated due to complexities occurring with the automatic mesh program. The load was applied under the head of the screw just as the tie plate would apply load to the screw spike.

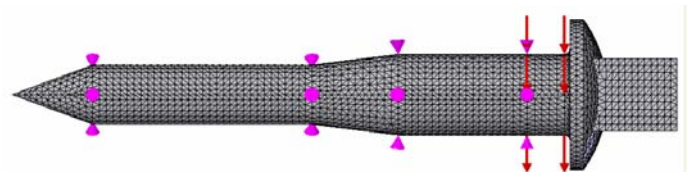


Figure 9. Screw spike FEA model overview. The red arrows indicate the applied load. The magenta cones indicate the edges of the elastic foundation.

The wood tie was simulated as an elastic foundation. As testing indicated, support stiffness of a wood tie could range significantly. For this reason a sensitivity study was conducted of wood tie stiffness and resulting tensile stress. A plot of the sensitivity results is shown in Fig 10. Results of the sensitivity study concluded that a variance at high stiffness (greater than 500,000 lbs/in² [135.7 N/mm²]) would have a limited

effect on screw spike stress. However, slight variations at lower stiffness (lower than 500,000 lbs/in/in² [135.7 N/mm/mm²]) would create a much more significant change of screw spike stress. The FEA model predicted that a lateral load above 8,000 lbs (35.6 kN) would create stresses above the endurance limit, no matter what the tie stiffness. Likewise, a lateral load below 3,500 lbs (15.6 kN) would not create stresses above the endurance limit, no matter what the tie stiffness.

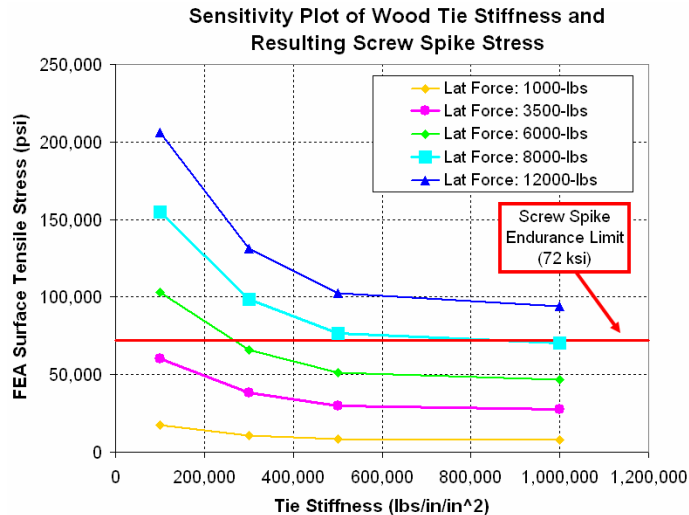


Figure 10. Results of sensitivity study of wood tie stiffness and resulting screw spike stress.

Figure 11 depicts the FEA model point of highest stress and an actual failed screw spike, which corresponded well with each other. Stress plots of the screw spike FEA model with an applied load of 6,000 lbs (26.7 kN) and three different tie stiffness values is shown Fig 12. Results concluded that a higher stiffness value moved the point of highest stress from the failure location to the shoulder of the screw and lowered the maximum stress. This would indicate that higher tie stiffness helps to support the screw spike at the shoulder and limit stresses at the failure location.

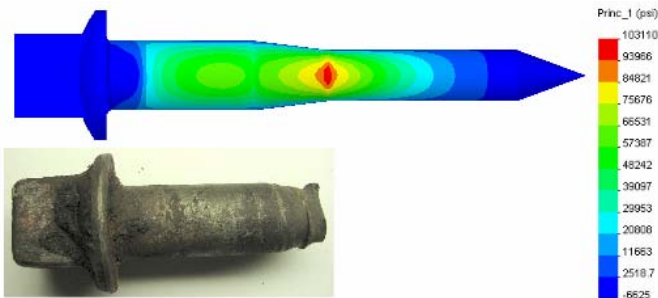


Figure 11. Point of highest tensile stress compared to location of screw spike fracture.

Applied Load: 6,000-lbs (26.7 kN)

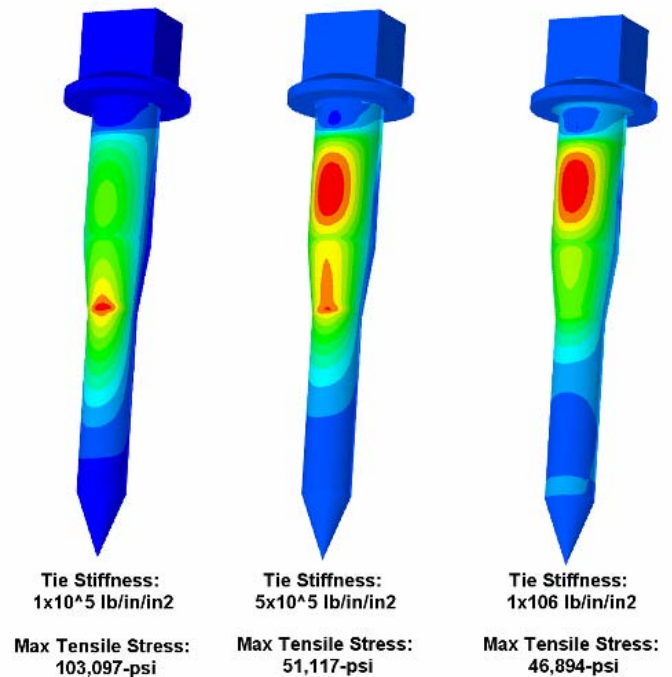


Figure 12. FEA results depicting effect of increased wood tie stiffness.

CONCLUSION

The goal of this research was to investigate the load environment and failure of screw spikes. Results of on-site testing concluded that not all four screw spikes within a tie plate carry an equal amount of load. One screw was found to carry 63.1% while another only carried 1.0%. Interestingly, these mismatched loads were on screw spikes directly opposite of each other on the field and gage side, respectively. Finite element analysis concluded that lateral loads exceeding 8,000 lbs (35.6 kN) would create stresses great enough to cause a fatigue fracture. Of all the instrumented screw spikes, only the screw that carried 63.1% of the tie plate load measured lateral loads in excess of 8,000 lbs (35.6 kN). Were that screw left in place, it is likely to have failed due to fatigue. It can be concluded that screw spike failures can be attributed to uneven division of lateral wheel loads among the screw spikes.

SUGGESTIONS FOR FUTURE WORK

The final conclusion of this research was that screw spike failures are a result of uneven loading between the screw spikes within a tie plate, specifically screw spikes that carry little to no load cause others to have excessive load. Little is known why this condition occurs. Further research should be conducted to determine the cause and remedy of this limited screw spike load capacity condition.

Designing a method to individually calibrate each screw spike on-site after it has been installed is highly recommended. This research discovered that the wood tie support stiffness to screw spikes can vary significantly, which greatly affects the calibration. Calibrating on-site would eliminate the issues with laboratory calibration.

Further testing should be conducted to investigate the long term effects of track thermal contraction on screw spike loads.

Results did indicate loading from track contraction on limited screw spikes; however a longer duration than 24-hours is needed to fully understand this loading condition.

Results of this analysis can be applied to redesign the screw spike to lower stresses at the failure location. Possibly a tie plate system can be designed to better control uneven loading between screw spikes.

Top of rail lubrication has been a popular method to reduce rail vehicle lateral wheel loads. Instrumented screw spikes can be used to compare loads with and without top of rail lubrication. This would help verify that top of rail lubrication can be used to help prevent screw spike failures.

ACKNOWLEDGMENTS

Dwight Clark with the Union Pacific Engineering Methods and Research Department and Union Pacific Railroad are gratefully acknowledged for their support of this research.